Combining Reflectometry and Fluorescence Microscopy: An Assay for the Investigation of Leakage Processes across Lipid Membranes

ARTICLE *in* ANALYTICAL CHEMISTRY · DECEMBER 2013

Impact Factor: 5.64 · DOI: 10.1021/ac4020726 · Source: PubMed

4 AUTHORS, INCLUDING:

Ingo Mey
Georg-August-Universität Göttingen
24 PUBLICATIONS **313** CITATIONS
SEE PROFILE

Claudia Steinem
Georg-August-Universität Göttingen
164 PUBLICATIONS **4,765** CITATIONS
SEE PROFILE

Andreas Janshoff
Georg-August-Universität Göttingen
204 PUBLICATIONS **5,630** CITATIONS
SEE PROFILE

analytical chemistry

Technical Note

pubs.acs.org/ac

Combining Reflectometry and Fluorescence Microscopy: An Assay for the Investigation of Leakage Processes across Lipid Membranes

Milena Stephan,[†] Ingo Mey,[‡] Claudia Steinem,[‡] and Andreas Janshoff*[,†]

[†]Institute of Physical Chemistry, University of Göttingen, Tammannstr. 6, Göttingen, Lower Saxony 37077, Germany

[‡]Institute of Organic and Biomolecular Chemistry, University of Göttingen, Tammannstr. 2, Göttingen, Lower Saxony 37077, Germany

Supporting Information

ABSTRACT: The passage of solutes across a lipid membrane plays a central role in many cellular processes. However, the investigation of transport processes remains a serious challenge in pharmaceutical research, particularly the transport of uncharged cargo. While translocation reactions of ions across cell membranes is commonly measured with the patch-clamp, an equally powerful screening method for the transport of uncharged compounds is still lacking. A combined setup for reflectometric interference spectroscopy (RIfS) and fluorescence microscopy measurements is presented that allows one to investigate the passive exchange of uncharged compounds across a free-standing membrane. Pore-spanning lipid membranes were prepared by spreading giant 1,2-dioleoyl-*sn*-glycero-3-phosphocholine (DOPC) vesicles on porous anodic aluminum oxide (AAO) membranes, creating sealed attoliter-sized compartments. The time-resolved leakage of different dye molecules (pyranine and crystal violet) as well as avidin through melittin induced membrane pores and defects was investigated.

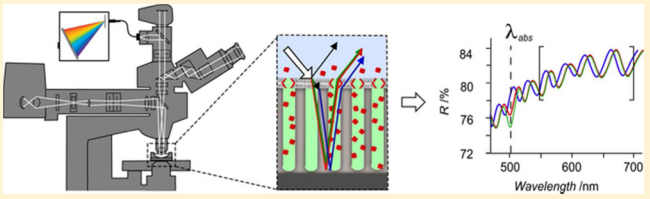

Biological membranes sustain concentration differences of biomaterials in cells compared to their immediate external surroundings, confine chemical reactions to a distinct space, or serve as a barrier to separate reactive agents, thus allowing cells to conduct necessary biochemical reactions in a highly controlled manner.[1] However, the separation cannot be absolute. In order for cells to maintain energy production, biosynthesis, and communication with their environment, they are critically dependent on uncharged molecules and ions being exchanged across this barrier.[2] An in depth understanding of the complex functions orchestrated by the cell membrane, thus, depends on methods capable of probing the active and passive passage of solutes across biological membranes. Since the majority of today's drugs are designed to influence such transport processes, these methods also play a key role in the drug discovery process.

The translocation reactions of ions across natural cell membranes or cell-membrane mimics are commonly measured by patching the lipid-bilayer with a small-scale pipet, in a way that electrical contact is obtained at each side of the membrane.[3] This electrophysiological technique known as the patch-clamp allows the recording of the currents of single ion channels.[4] Alternative electrical assay technologies, such as membrane potential, ion flux, and ligand displacement, have been developed to provide the capability to screen large compound libraries.[5,6] All of the above-mentioned electrical methods, albeit very powerful, share the inherent disadvantage that they are limited to measuring only the passage of charged compounds.[7]

Current assay formats aiming to elucidate the transfer of uncharged compounds, or the permeability of a membrane, utilize liposomes in solution or adsorbed on a surface and sense the translocation of a method specific probe molecule.[8−10] Detection of such sensor schemes relying on floating liposomes may be based on electrical readout, light scattering, or fluorescence spectroscopy. In a light scattering-based approach, the passage of a compound across the lipid membrane of a vesicle can be measured, since variations in scattered light intensity arise as the dimensions of the vesicle change in response to osmotically induced water transfer.[8] A secondary effect is related to solute passage, and therein lies the apparent limit of the assay, even though it is a labelfree method.[11] To measure membrane permeability, the most common approach involves the use of self-quenching fluorescent molecules such as carboxyfluorescein or calcein trapped in the interior of a liposome.[9] These probe molecules show an increase in fluorescence intensity, when released to the exterior; thus, an estimation of the permeability is obtained by measuring the time dependent change in fluorescence. However, these measurements often suffer from high background noise and perturbations of the translocation process due to the necessary high label concentration.

Transport assay formats relying on immobilized vesicles have been developed on the basis of attenuated total reflectance (ATR)-FT-IR, surface plasmon resonance (SPR), fluorescence,

Received: July 8, 2013
Accepted: December 30, 2013
Published: December 30, 2013

   dx.doi.org/10.1021/ac4020726 | *Anal. Chem.* 2014, 86, 1366−1371

and second harmonic signal generation (SHG) spectroscopy.[8−10,12] All of the listed techniques involve challenging preparation steps, since intact vesicles need to be immobilized on a substrate without providing the means to validate the surface preparation or choose the measurement site. Furthermore, the vesicles need to be filled with a probe molecule beforehand, and the available number of suitable molecules is limited.

In this study, we present a chip-based leakage assay format that aims to overcome some of the mentioned disadvantages of the current liposome-based methods. Surface-based bioanalytical sensor technologies offer the possibility to rapidly screen multiple events either sequentially or simultaneously. The emerging importance of these sensors in the field of life science stems from their compatibility with microfluidic handling, which allows measurements with small sample volumes and multiplexing rendering them ideally suited for studies of substances that are rare or time-consuming and expensive to obtain.[2]

Here, we present an optical approach, which does not necessarily rely on fluorescent probes and permits one to monitor the kinetics of the leakage processes across lipid membranes locally. The passage of two small dye molecules and a large protein through lipid membranes suspended on a porous substrate was simultaneously measured by absorption spectroscopy and reflectometric interference spectroscopy (RIfS) in a combined setup with fluorescence microscopy. Pore-spanning lipid membranes were prepared by spreading giant unilamellar vesicles (GUV) consisting mainly of 1,2-dioleoyl-*sn*-glycero-3-phosphocholine (DOPC) on orthogonally functionalized anodically etched aluminum oxide (AAO) chips. The potential of this assay is demonstrated by measuring the passive passage of molecules through membrane patches, which were made permeable by the action of melittin, the major constituent of bee venom.[13] Melittin is a small, cationic, and amphiphilic peptide composed of 26 amino acid residues.[14] Because of its amphiphilic nature, the peptide is water-soluble while simultaneously being capable of spontaneously associating with lipid membranes. At low concentrations, melittin binds to the outer layer of a membrane.[15] After a certain peptide-to-lipid threshold concentration is reached, melittin helices associate and lead to the formation of oligomeric pores. Depending on the experimental condition, pore sizes ranging from 1 to 6 nm have been reported.[15] The continued incorporation of melittin in the bilayer leads to the formation of larger pores with more monomers constituting its rim. At a high enough concentration, melittin has a lytic effect on cells.[16]

EXPERIMENTAL SECTION

Materials. 1,2-Dioleoyl-*sn*-glycero-3-phosphocholine (DOPC) was purchased from Avanti Polar Lipids, Inc. *N*-(Texas Red sulfonyl)-1,2-dihexadecanoyl-*sn*-glycero-3-phosphoethanolamine (TexasRed-DHPE) was acquired from Biotium (Hayward, California, USA). Aluminum in 99.999% purity was purchased from GoodFellow (Coraopolis, Pennsylvania, USA). Common chemicals as well as pyranine, melittin, crystal violet, and avidin from egg white were purchased from Sigma Aldrich (Deisenhofen, Germany).

Preparation of AAO Chips. Details on the production and functionalization of AAO transducer chips can be found in the Supporting Information and previous publications.[13,17,18] In short, aluminum substrates were electropolished by being submerged in a mixture of phosphoric and sulfuric acid. The polished chip was then electrochemically etched in oxalic acid in a two step process, resulting in an aluminum chip covered with a 3 μm thick layer of porous alumina (pore diameter 60 nm). The retained AAOs were functionalized via gas phase silanization with mercaptopropyl-triethoxysilane. The pore rims were covered with a protective layer of gold to allow for the removal of the functionalization inside the pores by plasma treatment.

Preparation of Pore-Spanning Lipid Membranes. Prior to measurement, the gold layer was removed with iodine solution and the pore rims were activated by an oxygen plasma treatment rendering them hydrophilic. The thus prepared chip was placed in 2 mL of buffer solution consisting of 20 mM HEPES, 100 mM NaCl, and 10 mM pyranine at pH 7.0. A lipid membrane was created on top of the AAOs, sealing the pores by spreading giant vesicles on top. For this purpose, 40 μL of a 0.25 mg/mL GUV solution was added to the chip. The vesicles consisting of DOPC doped with 1 mol % TexasRed-DHPE were prepared via gentle hydration in 0.3 M sucrose solution by storing them overnight in an oven at 50 °C.

Combined RIfS and Fluorescence Microscopy Setup. To create a combined setup for reflectometry and fluorescence microscopy, a BX51 fluorescence microscope (Olympus, Hamburg, Germany) was modified as follows. An iris diaphragm (CVI Melles Griot, Albuquerque, USA) and a 50/50 beam splitter (Ocean Optics, Dunedin, USA) were introduced into the beam path. Light is coupled from the beam splitter into an optical fiber (d = 1 μm) which guides it partly to the spectrometer (Nanocalc 2000 Vis/NIR, Ocean Optics, Dunedin, USA) and partly into the CCD camera (Infinity 2, Lumenera Corporation, Ottawa, Ontario, Canada). An ultrahigh power white light LED lamp (UHP-mic-LED-white, Prizmatix, Modiin-Ilite, Israel) was used as light source, since its emission is more stable than that of a mercury short arc. Before each measurement, the aperture diaphragm of the microscope was set to obtain the optimal interference signal from the objective currently used. A sketch of the setup and the RIfS signal obtainable with a 20× waterimmersion objective can be found in the Supporting Information, as well as information relating to the limit of detection of this combined setup.

Execution of Leakage Measurements. The experiments were carried out with the combined RIfS-microscope setup using a 20× water-immersion objective (UApo N 340, Olympus). Pore-spanning lipid membranes were prepared prior to measurement in pyranine solution to seal a fluorescent dye in the pores of the AAO film for two reasons. Pyranine serves as an indicator for successful membrane sealed compartments and also serves as a reporter dye for the efflux of molecules across the pore-spanning lipid bilayer. The sample was rinsed until no pyranine fluorescence remained in the solution above the transducer chip. A sufficiently large and defect-free membrane patch of adequate size was chosen, and images were taken of the red fluorescent bilayer above, as well as of the green fluorescent liquid in the pores (Figure 2B,C). The iris diaphragm was adjusted to allow only light reflected from pores sealed with lipid membrane to pass through to the spectrometer (white circle in Figure 2B). The measurement of white light reflectivity spectra was initiated by recording a baseline in buffer. Once stability of the signal was confirmed (usually after 5 min), the transducing agent was added to the measurement chamber (for avidin, c = 3 μM; for crystal violet, c = 200 or 500 nM). After the signal stabilized again, melittin was added (1 μM in all experiments). Eventually, the measurement

dx.doi.org/10.1021/ac4020726 | *Anal. Chem.* 2014, 86, 1366−1371

of reflectivity spectra was terminated, and once again, fluorescence images of the membrane and pore content were recorded.

Data Analysis. Depending on the experiment, reflectivity spectra were evaluated either to generate a time trace of the optical thickness change of the employed transducer chip (RIfS) or to track the reflectivity values at the absorption maximum (λ_{abs}) of the dye used as reporter molecule (pyranine: λ_{abs} = 450 nm; crystal violet: λ_{abs} = 590 nm). RIfS data (optical thickness) were generated from a wavelength range far away from the adsorption maximum of pyranine (500−600 nm).

RESULTS AND DISCUSSION

Reflectometric interference spectroscopy is based on the interference of white light-beams partially reflected on different interfaces of a thin transparent film. The modulation of the interference pattern depends on the angle of incidence and the wavelength of radiation, as well as on the optical thickness of the transparent layer, which is given by the product of the refractive index of the material and its physical thickness. Any change in or at the transparent film thus results in a wavelength-shift in the interference spectrum. This effect is shown in Figure 1B,C and can be utilized to measure the deposition of material on a transducer chip and is a well-known label-free detection concept in biosensing.[19,20]

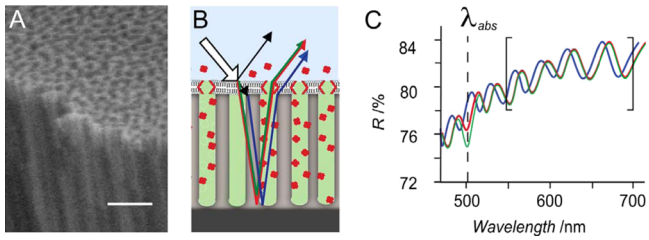

Figure 1. (A) SEM image of AAO chip (scale bar 500 nm). (B) Schematic drawing of the sensing principle. Adsorption of an agent (red dots), that passed the membrane on the chip walls, leads to a change of the refractive index of the AAO membrane. The change of the refractive index results in a red-shift of the interference pattern (C: blue to red curve). A dye entrapped under the membrane (green area) or entering the porous layer from the outside attenuates the reflectivity of the chip at the absorption maximum of the dye (green curve shown in C).

In order to measure the passage of molecules across a lipid membrane locally, a very small measurement area is chosen. This is difficult to achieve with other label-free optical methods, which mostly integrate over a larger region of interest. Label-free optical techniques such as RIfS all share one main disadvantage compared to sensing methods relying on tagged compounds. Their measured signal is averaged over a relatively large surface area or volume fraction which, very often, may not even be chosen by the user, meaning that, for example, defective surface functionalizations can have a detrimental effect on the outcome of an experiment. A solution to this problem can be to combine the technique with optical microscopy that permits one to chose a region of interest displaying the best surface properties. By coupling RIfS with an upright fluorescence microscope, we gained access to sensing areas as small as 10 μm^2. An ultrahigh power white LED, whose emission spectrum is more stable than that of a mercury short arc, was chosen as a light source for both producing interference fringes and fluorescence. It was not possible to generate a decent white light interference spectrum from an objective with a numerical aperture (NA) higher than 0.3. As was stated earlier, the modulation of an interference spectrum is angle dependent. Objectives with NA > 0.3 gather light over a wide range of collection angles, meaning that different path lengths correspond to destructive or constructive interference for the same wavelength; thus, interference fringes are no longer visible in the spectrum. To still be able to measure RIfS with objectives of NA > 0.3, the lateral irradiation of the surface needed to be limited, to efficiently restrict the angles of light collection. This was achieved with the aperture diaphragm, a standard component of every microscope. The exchange of the light source combined with the use of the diaphragm leads to lower illumination light intensity, something that would be considered a drawback in investigations based on fluorescence but proved to be important in long-term kinetic measurements, since bleaching of the employed dyes is largely avoided. The sensing limits of the combined RIfS fluorescence microscopy setup compared to conventional RIfS were determined by performing protein binding (streptavidin−biotin) studies on lipid membranes deposited on silica wafers with a thick oxide layer to generate interference fringes. Information concerning limit of detection of measurements with different objectives can be found in the Supporting Information.

The basic sensing concept of the leakage assay is illustrated in Figure 1. Pore-spanning membranes are created on AAO chips by spreading giant vesicles on the orthogonally functionalized substrate. The pore-spanning lipid membrane entraps pyranine in the pores (Figure 1B, green area) confirming that the cavities are indeed sealed by the lipid membrane. The presence of an absorbing agent such as pyranine in the AAO chip leads to an attenuation of its reflectivity (at the absorption maximum of that compound, Figure 1C), since the absorbing agent affects the complex effective refractive index (extinction coefficient) of the porous transducer. This phenomenon was used to detect the passage of dyes in and out of the membrane covered area. Additionally, the adsorption of material on the pore walls of the AAO chip can be monitored simultaneously by following the shift of the interference fringes to higher wavelengths (red shift). We used this detection scheme, comprising alterations in both the optical thickness and the reflectivity of the alumina chip, to sense the passive passage of solutes of different sizes through the lipid membrane permeabilized by addition of melittin from solution.

Investigating the Leakage of Small Molecules. This experiment allows one to investigate the action of pore-forming peptides that generate pores and defects in lipid bilayers by observing the leakage of small dye molecules in and out of the membrane covered areas. In the measurement shown in Figure 2, the entry of molecules into the pores of the AAO chip was measured using the triphenylmethane dye crystal violet as a nonfluorescent reporter molecule. Prior to measurement, AAO pores were sealed by spreading GUVs labeled with TexasRed on the substrate. By means of fluorescence microscopy, a suitable measurement site was identified on the porous alumina substrate (Figure 2B,C: fluorescence in green and red indicates well sealed compartments), and the region of interest for RIfS was limited to an area that appears to be entirely covered by the membrane (Figure 2B: white circle) to minimize leakage from the borders of the patch or adjacent defects. The fluoresence image of the TexasRed labeled membrane shown in Figure 2B

dx.doi.org/10.1021/ac4020726 | Anal. Chem. 2014, 86, 1366−1371

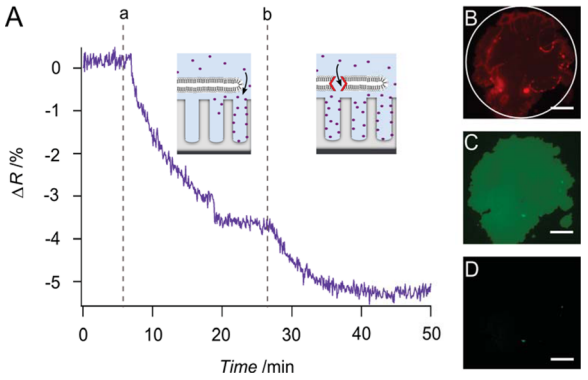

Figure 2. Diffusion of crystal violet through pores and defects of pore-spanning lipid bilayers sealing alumina pores. (A) Time trace of the reflectivity values recorded at the absorption maximum of crystal violet (λ_{abs} = 590 nm; violet curve). At point "a", crystal violet was introduced to the system (c = 500 nM) comprising alumina pores covered with lipid bilayers originating from spread GUVs. When the signal stabilized, melittin was added at point "b" (c = 1 μM). (B) Fluorescence image of the Texas Red labeled lipid membrane patch. The white circle indicates position of aperture diaphragm. (C) Fluorescence image of pyranine entrapped in the pores at the beginning of the experiment. (D) Same image as C at the end of the measurement. The pyranine fluorescence is completely gone (scale bars: 20 μm).

shows inhomogeneities in fluorescence intensity. These arise from the spreading process of GUVs. The rim of the membrane patch adopts folded edge structures with nonbilayer structure, leading to higher fluorescence intensity in those areas.[21] The time trace shown in Figure 2A was generated by tracking the reflectivity values at the absorption maximum of crystal violet (590 nm) that was added to the outer solution at point "a", causing the reflectivity to decrease immediately. This effect may be attributed to dye molecules entering some pores and adsorbing on surfaces that are not covered by a lipid membrane. Once the signal saturated, melittin (c = 1 μM) was introduced to the system (point "b") which lead to a second drop in the measured signal. The further decrease of the reflectivity was most likely caused by the formation of melittin induced pores inside the lipid patch that allowed dye molecules to enter into alumina pores which were previously sealed by a lipid membrane. At the beginning and the end of the experiment, fluorescence images of the pore content were taken (Figure 2C,D). Figure 2D shows that the pyranine fluorescence vanished from the interior of the pores, indicating that the content of the cavities was exchanged and thus that the membrane was indeed made permeable by melittin addition.

Generally, it should not be possible to measure the absorption of dissolved crystal violet in a concentration as low as 500 nM in the porous matrix. This is verified by calculating the Fresnel coefficients of light reflected and transmitted at the interfaces of our sensor assembly:

$$r_{12} = \frac{n_1 - n_2}{n_1 + n_2} \qquad (1)$$

$$t_{12} = \frac{2n_1}{n_1 + n_2}$$

where n_1 indicates the refractive index of the ambient medium (water) and n_2 is the refractive index of the AAO membrane. n_2 becomes a complex quantity $n_2 = n_{eff} - ik_{eff}$, once crystal violet diffuses into the pores. n_{eff} and k_{eff} may be calculated according to an effective medium approximation introduced by Garahan et al.[22] Their model predicts the effective index of refraction and absorption index of nanoporous thin films. The equations given below are valid for horizontally aligned cylindrical nanopores with different diameters and various porosities.

$$n_{eff}^2 = \frac{1}{2}(A + \sqrt{A^2 + B^2}) \qquad (2)$$

$$k_{eff}^2 = \frac{1}{2}(-A + \sqrt{A^2 + B^2})$$

with

$$A = f(n_d^2 - k_d^2) + (1 - f)(n_m^2 - k_m^2) \qquad (3)$$

and

$$B = 2n_d k_d f + 2n_m k_m (1 - f) \qquad (4)$$

f denotes the filling factor of domains present in the substrate, n_m is the refractive index of the substrate material, and n_d is the refractive index of the material forming the domains. Having calculated the refractive index of the porous layer and the Fresnel coefficients of the system, its reflectivity R may be estimated according to:

$$R = \left(\frac{r_{12} + r_{23} e^{-2i\delta}}{1 - r_{21} r_{23} e^{-2i\delta}} \right)^2 \qquad (5)$$

with

$$\delta = \frac{2\pi}{\lambda} d n_2 \qquad (6)$$

the phase difference between the reflected and refracted light-beam. We found that, for a dye such as crystal violet with an extinction coefficient of 1.4×10^4 M^{-1} cm^{-1}, to cause a change in reflectivity of 5% as the one shown in Figure 2A, its concentration inside the pores would have to be at least 20 mM.[23] The high change in reflectivity may be explained by the fact that triphenylmethane dyes are known to adsorb on alumina, meaning crystal violet molecules accumulate on the pore walls of the transducer chip leading to higher local concentrations.[24] A concentration as high as 20 mM would mean that 100 000 molecules are present in each pore. Relating this number to the available wall area of 56 000 nm^2 per pore shows that the chip surface is almost completely covered with crystal violet at the end of the experiment. Kinetics of AAO pore filling through passive diffusion was simulated by finite elements (Supporting Information). The simulations show that the rate limiting step is adsorption of the solute on the pore walls rather than the defect size in the bilayer. Kinetics are further slowed down due to depletion of crystal violet in the supernatant which can be attributed to the high surface area sweeping out the molecules once they entered the pores. It was described in the previous experiment how the leakage of a dye from the outer medium into the pores of the chip may be measured, and Figure 3 shows that it is also possible to measure the passage of the entrapped fluorescent dye pyranine to the ambient medium.

The time trace shown in Figure 3A was generated by tracking the reflectivity value of the absorption maximum of pyranine (450 nm) with time. At point "a", melittin (c = 1 μM) was introduced to the system. After a lag time of approximately 8 min, an increase in the measured signal can be seen. This

dx.doi.org/10.1021/ac4020726 | Anal. Chem. 2014, 86, 1366−1371

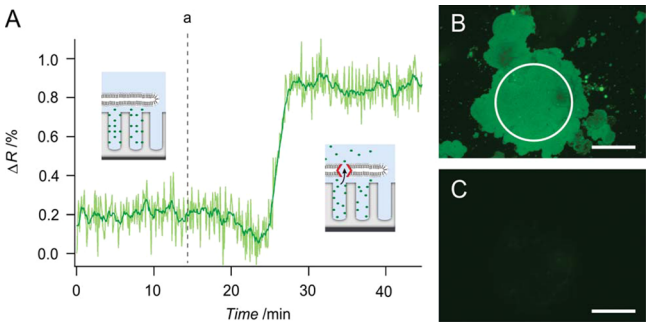

Figure 3. Efflux of entrapped pyranine from membrane covered pores. (A) Time trace of the reflectivity values for the absorption maximum of pyranine (c = 10 mM; A_{max} = 450 nm; green curve). For better presentation, data was smoothed by averaging over 5 data points. (Original data is shown in lighter color.) At point "a" melittin was added to the system (c = 200 nM). (B) Fluorescence image of pyranine entrapped in the pores at the beginning of the experiment. The white circle indicates position of aperture diaphragm. (C) Same image as (B) at the end of the measurement. Pyranine fluorescence has vanished (scale bars: 50 μm).

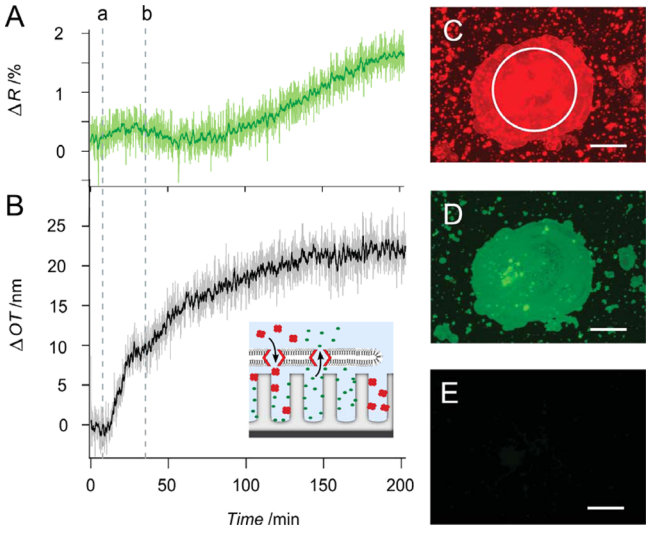

Figure 4. Passage of avidin through melittin induced defects in a pore spanning membrane. (A) Time trace of the reflectivity values for the absorption maximum of pyranine (450 nm; c = 10 mM). At point "a", avidin was introduced to the system (c = 3 μM). When the OT stabilized, melittin was added at point "b" (c = 1 μM). (B) Change of optical thickness of porous AAO membrane during avidin adsorption on the pore walls. (C) Fluorescence image of TexasRed labeled membrane on top of the AAO chip. The white circle indicates position of aperture diaphragm. (D) Fluorescence image of pyranine entrapped in the pores at the beginning of the experiment. (E) Same image as (D) recorded at the end of the measurement. No pyranine fluorescence can be detected (scale bars: 50 μm). To highlight characteristic features of the curves, the original data (shown in lighter color) was smoothed by averaging over 5 data points.

indicates the outward flow of pyranine molecules and therefore the formation of melittin pores in the lipid membrane which are large enough to allow the molecules to leave the pores by crossing the bilayer. The fluorescence images shown in Figure 3B,C strengthen this interpretation since the pyranine fluorescence has almost completely vanished at the end of the experiment (Figure 3C).

The observed retardation of the reflectivity increase indicating the leakage of pyranine out of the pores may originate from the fact that the highly negatively charged pyranine sticks via electrostatic interaction to the pore walls of the AAO. The desorption kinetics of pyranine leaving the pore walls may be considerably slowed down due to rebinding of the released molecules to free surface sites. This reduces the bulk concentration of pyranine in the pores and therefore also reduces the gradient that drives the dye molecules out of the pore. The length of the narrow pores leads to a tremendous number of surface contacts of the released molecules, while diffusing out of the cavity, and thus increases the probability of sticking of the dye after desorption, and hence reduces the desorption kinetics accordingly. The flux out of the pores is time dependent, since the concentration gradient changes with time and displays a maximum. The flux increases with time, because the bulk concentration in the pore increases, due to the growing number of pyranine molecules desorbing from the pore walls. A detailed discussion and finite elements simulations showing a retarded release of adsorbent from pores after flushing the supernatant are previously provided by Lazzara et al.[17] In summary, the high surface area of the porous substrate and the small entrance area lead to a high rebinding probability of pyranine which in turn increases the dwell time of the dye inside the pores.[17]

It is also possible to measure efflux and influx of two different dyes simultanously as shown for crystal red and pyranine in the Supporting Information. It is, however, important that the two absorption maxima are sufficiently separated from each other.

Investigating the Leakage of Large Solutes. The passage of large solutes such as proteins and peptides through lipid membranes may be sensed directly and label-free via reflectometric interference spectroscopy as demonstrated in Figure 4. As in the previous experiment, a pore-spanning lipid membrane preparation with pyranine enclosed in the cavities of the AAO chip is used (Figure 4C,D). At point "a", avidin was added to the system (Figure 4A,B). Avidin readily adsorbs on AAO membranes at a pH > 3.[17] The adsorption of avidin on those parts of the transducer chip that were not sealed by a lipid membrane led to an increase in OT of 10 nm. After the signal saturated, melittin was added, upon which the optical thickness started to rise again.

The graph shown in Figure 4A shows again a lag phase for the outward leakage of pyranine as compared to the inward leakage of avidin (Figure 4B). The fluorescence image taken at the end of the experiment (Figure 4E) proves that pyranine has left the cavities completely. Compared to leakage of crystal violet into the pores followed by adsorption on the pore walls, avidin influx is slower, which is due to a smaller adsorption rate. Melittin first adsorbs on the membrane and once a certain lipid protein ratio is reached, it starts to insert in the membrane and to assemble into structures creating defined pores in the lipid bilayer.[16] The accumulation of melittin leads to the formation of a higher number of pores and enlarges their size, thus eventually allowing more of the rather bulky avidin molecules to pass the lipid bilayer.[15] This process may finally lead to the breakdown of the lipid bilayer structure even though an effect on the fluorescence of the membrane was not observable (Supporting Information).

Taken together, applying RIfS to local areas of the surface allows one to investigate the passage of a reporter molecule through the membrane by binding to the pore walls of the transducer chip. This works without the need of a fluorescent

dx.doi.org/10.1021/ac4020726 | Anal. Chem. 2014, 86, 1366−1371

label that could be detrimental to the biological activity of the compound and is readily bleached.

CONCLUSION

We showed that a setup combining RIfS with optical microscopy can be realized with very low technical effort and offers many advantages comprising the obvious benefit of direct visual confirmation of the outcome of the experiment and the possibility to actively choose the area to be investigated by monitoring binding events and considerably smaller measurement sites (approximately 10 μm^2 compared to 1 mm^2). Furthermore, we showed that, with this sensor assembly, it is possible to monitor the leakage in and out of a membrane covered cavity individually and simultaneously via absorption spectroscopy and RIfS. Compared to common leakage assays and other sensors to monitor transport of uncharged cargo, our setup allows one to locally address a specific membrane area as a specific region of interest. Importantly, the experiment does not necessarily rely on bulky and readily bleached fluorescent dyes that are usually used in high concentration to obtain self-quenching conditions. A reporter molecule in this assay needs to fulfill one criterion, it has to affect the complex refractive index of the porous alumina chip. This can be achieved by administration of either large enough molecules such as avidin or small chromophores that display appreciable absorption. For absorption measurements as demonstrated with the crystal violet and the pyranine measurement, the choice of reporter molecules is only limited to the fact that their absorption maximum needs to be somewhere in between the mid UV to near IR spectrum. This results in a very high number of possible probe molecules posing an obvious advantage of this assay to conventional fluorescence-based leakage assays that rely on self-quenching fluorescent dyes, which require high dye concentrations and are readily perturbed by photobleaching.

This rather straightforward assay format holds an incredible wealth of possible future applications. For example, since the sensor allows one to detect different reporter molecules labeled or unlabeled simultaneously, a dynamic pore formation process as the one of melittin or other pore-forming peptides such as caerin, magainin, or ascaphin can be elucidated simultaneously based on the size of the different reporter molecules. AAOs offer a large library of different surface functionalizations. By equipping the inner pore walls with a specific receptor, the passage of the corresponding partner through a lipid membrane could be monitored. Additionally, the sensor is not limited to artificial membrane systems. The investigation of whole cells or cell membrane fragments could be feasible as well.

ASSOCIATED CONTENT

Supporting Information

Additional information as noted in text. This material is available free of charge via the Internet at http://pubs.acs.org.

AUTHOR INFORMATION

Corresponding Author

*E-mail: ajansho@gwdg.de.

Notes

The authors declare no competing financial interest.

ACKNOWLEDGMENTS

We want to thank Dr.Thomas D. Lazzara for sharing his knowledge of AAO preparation with us. Financial support from SFB 937 (A8) is gratefully acknowledged.

REFERENCES

(1) Cardenas, A. E.; Jas, G. S.; DeLeon, K. Y.; Hegefeld, W. A.; Kuczera, K.; Elber, R. *J. Phys. Chem. B* **2012**, *116*, 2739−2750.
(2) Ohlsson, G.; Tabaei, S. R.; Beech, J.; Kvassman, J.; Johanson, U.; Kjellbom, P.; Tegenfeldt, J. O.; Höök, F. *Lab Chip* **2012**, *12*, 4635−4643.
(3) Hamill, O. P.; Marty, A.; Neher, E.; Sakmann, B.; Sigworth, F. J. *Pflügers Arch.* **1981**, *391*, 85−100.
(4) Neher, E.; Sakmann, B. *Nature* **1976**, *260*, 799−802.
(5) Treherne, J. M. *Curr. Pharm. Des.* **2006**, *12*, 397−406.
(6) Zheng, W.; Spencer, R. H.; Kiss, L. *Assay Drug Dev. Technol.* **2004**, *2*, 543−552.
(7) Guidelli, R.; Becucci, L. *J. Solid State Electrochem.* **2011**, *15*, 1459−1470.
(8) Cohen, B. E.; Bangham, A. D. *Nature* **1972**, *236*, 173−174.
(9) Chen, P. Y.; Pearce, D.; Verkman, A. S. *Biochemistry* **1988**, *27*, 5713−5718.
(10) Chen, C.; Tripp, C. P. *Biochim. Biophys. Acta* **2008**, *1778*, 2266−2272.
(11) Verkman, A. S. *J. Membr. Biol.* **1995**, *148*, 99−110.
(12) Brändén, M.; Dahlin, S.; Höök, F. *ChemPhysChem* **2008**, *9*, 2480−2485.
(13) Lazzara, T. D.; Carnarius, C.; Kocun, M.; Janshoff, A.; Steinem, C. *ACS Nano* **2011**, *5*, 6935−6944.
(14) Terwilliger, T. C.; Eisenberg, D. *J. Biol. Chem.* **1982**, *9*, 6010−6015.
(15) Kokot, G.; Mally, M.; Svetina, S. *Eur. Biophys. J.* **2012**, *9*, 461−474.
(16) van den Bogaart, G.; Velasquez Guzman, J.; Mika, J. T.; Poolman, B. *J. Biol. Chem.* **2008**, *283*, 33854−33857.
(17) Lazzara, T. D.; Mey, I.; Steinem, C.; Janshoff, A. *Anal. Chem.* **2011**, *83*, 5624−5630.
(18) Lazzara, T. D.; Behn, D.; Kliesch, T. T.; Janshoff, A.; Steinem, C. *J. Colloid Interface Sci.* **2012**, *366*, 57−63.
(19) Gauglitz, G.; Brecht, A.; Kraus, G.; Nahm, W. *Sens. Actuators, B: Chem.* **1993**, *11*, 21−27.
(20) Gauglitz, G. *Anal. Bioanal. Chem.* **2010**, *398*, 2363−2372.
(21) Kocun, M.; Lazzara, T. D.; Steinem, C.; Janshoff, A. *Langmuir* **2011**, *27*, 7672−7680.
(22) Garahan, A.; Pilon, L.; Yin, J. *J. Appl. Phys.* **2007**, *101*, 014320.
(23) Adams, E. Q.; Rosenstein, L. *J. Am. Chem. Soc.* **1914**, *36* (7), 1452−1473.
(24) Markovics, A.; Nagyb, G.; Kovacsa, B. *Sens. Actuators, B: Chem.* **2009**, *139*, 252−257.